Available online at www.sciencedirect.com
SCIENCE DIRECT®
Chemical Physics Letters 410 (2005) 282–287
CHEMICAL PHYSICS LETTERS
www.elsevier.com/locate/cplett

Enhancement of three-photon absorption cross-sections in a novel class of symmetrical charge transfer fluorene-based molecules

Wenbo Ma [a,*], Yiqun Wu [a,b], Junhe Han [c], Donghong Gu [a], Fuxi Gan [a]

[a] Department of Optical Storage, The Shanghai Institute of Optics and Fine Mechanics, The Chinese Academy of Sciences, Number 390, Qinghe Lu Road, Shanghai 201800, PR China
[b] Lab of Functional Materials, Heilongjiang University, Haerbin 150080, PR China
[c] Lab of Modern Optics, Department of Physics, Henan University, Kaifeng 475001, PR China

Received 18 January 2005; in final form 20 April 2005
Available online 16 June 2005

Abstract

The three-photon absorption effect (3PA) of two novel symmetrical charge transfer fluorene-based molecules (abbreviated as BASF and BMOSF) has been determined by using a Q-switched Nd:YAG laser pumped with 38 ps pulses at 1064 nm in DMF. The measured 3PA cross-sections are 84×10^{-78} and 114×10^{-78} $cm^6\ s^2$, respectively. The geometries and electronic excitations of these two molecules are systematically studied by PM3 and ZINDO/S methods. The relationships between 3PA cross-sections and intramolecular charge transfer are discussed micromechanically. The experimental and theoretical results have shown that the larger intramolecular charge transfer, which was characterized by the charge density difference between the ground state (S_0) and the first excited state (S_1), the greater enhancement of the 3PA cross-sections.

1. Introduction

In the early 1930s multiphoton absorption of an atom was introduced into the literature as a new concept by Göppert-Mayer [1] and it is becoming an intriguing subject in the chemistry, photonics, and biological imaging communities. Multiphoton absorption can be defined as simultaneous absorption of two or more photons through virtual states in a molecule or medium. More specifically, for a three-photon absorption (3PA) process, the cubic dependence of three-photon process on the incident light intensity provides a stronger spatial confinement, so that a higher contrast in imaging can be obtained than two-photon absorption (TPA) process [2–4].

Molecules with large 3PA cross-sections (σ_3') can be easily applied in the fields of multiphoton fluorescence imaging [5–7], up-converted stimulated emission [8], optical limiting [9–11] and light-activated therapy [12]. However, the relatively small σ_3' values of existing nonlinear organic molecules have deferred their practical applications. The development of molecules with large σ_3' values require more detailed studies on the structure–property relationships for nonlinear optics. Much effort of these studies on 3PA in organic molecules has been undertaken in recent years, for example, Hernández et al. [13] compared the 3PA cross-sections of two fluorene derivatives with donor-bridge-donor (D-π-D) and donor-bridge-acceptor (D-π-A) archetypes, the result was shown that symmetric intramolecular charge transfer in the D-π-D molecule enhances 3PA in these fluorene derivatives. Recently, theoretical and experimental investigations revealed [14,15] that a major contribution to the σ_3' values originates from the transition dipole moment from the ground state to lowest charge transfer excited state. Also, increasing the conjugation length and increasing the charge-transfer dimensionality would be valuable to enhance the 3PA cross-sections.

* Corresponding author. Fax: +86 21 69918800.
E-mail address: ma_wenbo@mail.siom.ac.cn (W. Ma).

0009-2614/$ - see front matter © 2005 Elsevier B.V. All rights reserved.
doi:10.1016/j.cplett.2005.04.116

In this Letter, we investigate a novel class of fluorene-based molecules with the same symmetric, D-π-D, conjugated structure, which are named as 4-(2-(7-(4-aminostyryl)-9,9-bis(2-ethylhexyl)-9H-fluoren-2-yl)vinyl) benzenamino (abbreviated as BASF) and 2,7-bis(4-methoxystyryl)-9,9-bis(2-ethylhexyl)-9H-fluorene (abbreviated as BMOSF). In an effort to gain insight into the effect of donor groups on the three-photon absorption properties of fluorene-based molecules, so as to provide useful information for the design of large three-photon absorbing materials. We use intensity dependent transmission measurement to obtain the three-photon absorption cross-sections of these two molecules at 1064 nm pumped with ps laser, and combined with the quantum chemistry calculations, we investigated the influence of intra-molecular charge transfer on three-photon absorption cross-sections in detail.

2. Experimental

2.1. Materials

These two molecules were synthesized by Pd-catalyzed Heck coupling reactions [16]. The chemical structures of the fluorene-based molecules under study are shown in the top-right corner in Fig. 1. In BASF and BMOSF the central fluorene is symmetrically end-capped with donor groups (amino group and methoxyl group, respectively) forming a D-π-D sequence. Elemental analysis, MS, IR spectrum and UV–VIS spectrum have identified the chemical structures of two molecules. The linear absorption spectrum and one-photon fluorescence spectrum were measured by using Lambada 9 UV/VIS/NIR recording spectrophotometer and FP-6500 fluorescence spectrometer, respectively. These two molecules solution in DMF with a concentration of 1.5×10^{-5} mol l^{-1} filled in a 1-cm-path quartz cuvette was used for both measurements.

2.2. Measurement of nonlinear transmission

In the measurement of nonlinear transmission, the incident 1064 nm lasing was provided by a Q-switched Nd:YAG laser (Continuum, PY61C-10) with pulse duration of 38 ps, repetition rate of 10 Hz. The laser beam was separated into two beams by the beam splitter (BS). The weaker beam, detected by a photodiode PD1, was used to monitor the incident laser energy. The stronger beam, being focused into the sample by a 25 cm focal-length lens, acted as the exciting beam. The entire transmitted intensities through the sample were totally collected to a photodiode PD2. These two photodiodes were connected with a two-channel energy meter (Molectron EPM 2000) to record the input and output energy simultaneously. Rotating a half-wave plate between two polarizers controlled the pump energy. The input energy was adjusted from low to high and corresponding output energy can be obtained simultaneously.

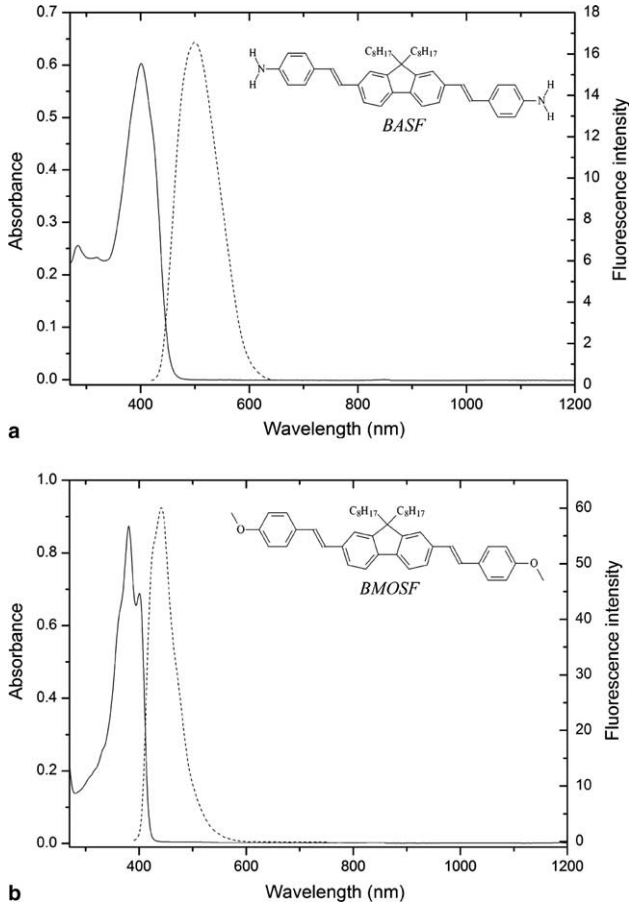

Fig. 1. Linear absorption (solid line) and one-photon fluorescence spectra (dash line) of BASF (a) and BMOSF (b) in DMF at a concentration of 1.5×10^{-5} mol l^{-1}.

2.3. Quantum chemistry calculations

The optimized geometries of two molecules and charge density distributions in both ground- and excited-state were calculated using PM3 semi-empirical method in the MOPAC quantum chemical package [17]. The excited states are characterized, and the electronic transitions are computed by ZINDO/S method [18,19] at the optimized geometries.

3. Results and discussion

3.1. Linear absorption and fluorescence emission

Fig. 1 shows the linear absorption and emission spectra of 4-(2-(7-(4-aminostyryl)-9,9-bis(2-ethylhexyl)-9H-fluoren-2-yl)vinyl)benzenamino (abbreviated as BASF)

and 2,7-bis(4-methoxystyryl)-9,9-bis(2-ethylhexyl)-9H-fluorene (abbreviated as BMOSF) in DMF solution. The both two molecules show strong UV absorption in the spectral range of 280–470 nm with absorption peak at 400 and 382 nm, respectively, which are all correspond to transitions $S_1 \leftarrow S_0$ [20]. There is no one-photon absorption for these two molecules in the entire near IR and most (>470 nm) of the visible spectral range. The three-photon energy of 1064 nm radiation just falls into the strong UV absorption, and therefore three-photon absorption in this solution may be expected. The one-photon fluorescence spectrums of two molecules are also shown in Fig. 1 by a dash line. One can find that the fluorescence band of these two molecules is located at blue–green region with the peak wavelength of 500 nm and 442 nm, respectively. Fluorescence quantum yields, Φ, were measured for BASF ($\Phi = 0.27$) and BMOSF ($\Phi = 0.44$) by a standard method relative to Coumarin 307 in methanol ($\Phi = 0.56$) [21].

3.2. Three-photon absorption cross-sections

Using intensity dependent transmission measurement we measured the three-photon absorption coefficients for both fluorene molecules in DMF solution with concentration of 0.03 mol l^{-1} at 1064 nm wavelength. In Fig. 2, the transmitted intensity as a function of the incident intensity is illustrated. The solid lines represent the theoretically fitted curve derived using basic theoretical considerations for three-photon absorption. Neglecting linear absorption at the pump wavelength, the intensity change of an excitation beam along the optical propagation path z is simply written as

$$dI(z)/dz = -\gamma I^3(z), \tag{1}$$

where γ is the three-photon absorption coefficient of the given sample medium. The solution of Eq. (1) can be simply obtained as [9]

$$I(z) = I_0/\sqrt{(1 + 2\gamma z I_0^2)}, \tag{2}$$

where I_0 is the incident intensity of the excitation beam. Eq. (2) is adequate for a cw incident beam or a pulsed beam with a rectangular temporal profile. In our case the incident pulses had a quasi-Gaussian temporal profile; therefore we could further assume an equivalent rectangular pulse shape to give a rough estimate of intensity I_0 or $I(z)$ [9]. From the relationship between $I(z)$ and I_0, the three-photon absorption coefficient γ can be easily deduced.

The γ values corresponding to the best fit are 4.34×10^{-20} and 5.92×10^{-20} cm^3 W^2 for BASF and BMOSF, respectively. Based on the known γ value of the measured solution sample, the molecular absorption cross-section σ_3' (in the units of cm^6 s^2) for given sample in solution is obtained by [13]

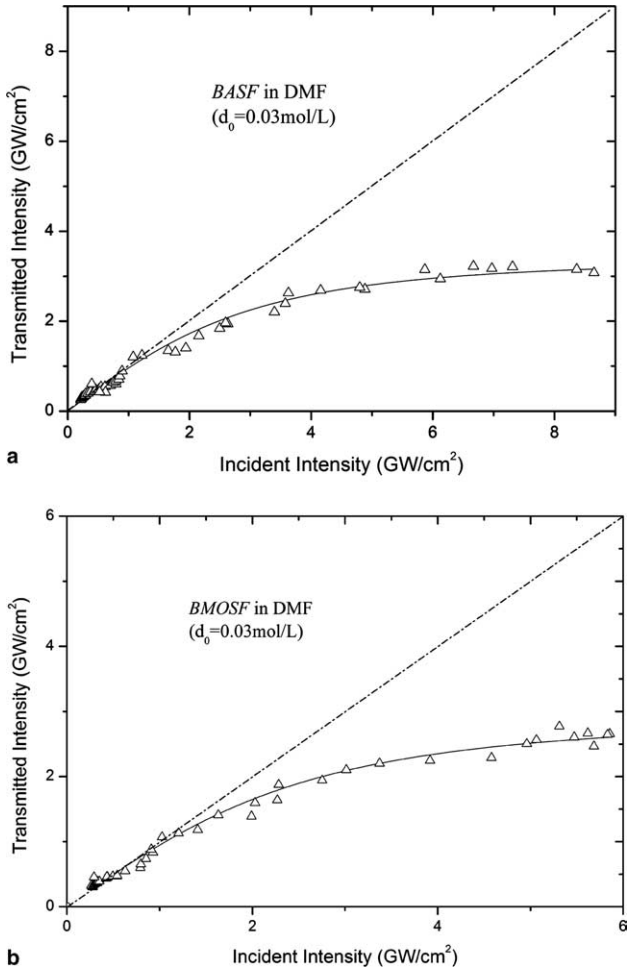

Fig. 2. Transmitted intensity versus input intensity of BASF (a) and BMOSF (b) in DMF at 0.03 mol l^{-1}. The solid lines are the theoretical best-fit curve with the parameter of $\gamma_{BASF} = 4.34 \times 10^{-20}$cm^3 W^2 and $\gamma_{BMOSF} = 5.92 \times 10^{-20}$cm^3 W^2. The linear dashed lines correspond to the data for pure DMF.

$$\sigma_3' = \frac{\gamma}{N_A \cdot d_0 \times 10^{-3}} \left(\frac{hc}{\lambda}\right)^2. \tag{3}$$

Here, N_A is Avogadro constant, d_0 is the concentration of the sample in solution (in the units of mol l^{-1}), and $h(c/\lambda)$ is the energy of an incident photon at 1064 nm. So the intrinsic sample molecular σ_3' values can be easily estimated as 84×10^{-78} and 114×10^{-78} cm^6 s^2 for BASF and BMOSF, respectively. Due to the influence of the quartz and the uncertainty of the incident intensity, the final results of γ and σ_3' of these two molecules have an experimental uncertainty of 10%.

The values of σ_3' for these two symmetric fluorene-based molecules are in the same order of magnitude for reported symmetric homologous ($\sigma_3' = 82 \times 10^{-78}$ cm^6 s^2), and significantly larger than that for the reported asymmetric homologous ($\sigma_3' = 37 \times 10^{-78}$ cm^6 s^2) [13]. This result indicates that symmetric intramolecular charge transfer in the D-π-D molecule certainly helps to enhance 3PA in these fluorene-based molecules which is in agree-

ment with the conclusion of Hernández et al. But whether the donor strength makes contribution to the enhancement of 3PA cross-sections is not discussed in existing literatures to the best of our knowledge, so it is significative to make clear the influence of intra-molecular charge transfer on three-photon absorption cross-sections.

3.3. Electronic excitations and intramolecular charge transfer

The ZINDO/S semi-empirical method has been used to obtain the nature and the energy of the first 10 singlet–singlet electronic transitions of the two molecules at the PM3 optimized geometry. The Electronic transition data are shown in Tables 1 and 2. It can be seen that the oscillator strength (f) and the transition dipole moment along the long axis of the molecule (X) of the $S_0 \rightarrow S_1$ electronic transition are the largest, which indicated that the excitation scheme for these two molecules is dominated by the transition to the first excited state, and excitation to the S_1 state corresponds almost exclusively to the promotion of an electron from the HOMO to the LUMO, which are both delocalized over the whole molecule. Recently, theoretical investigation revealed that there are more possible transition paths from ground to final states, S_f, involved in a three-photon absorption process, such as (I) $S_0 \rightarrow S_i \rightarrow S_j \rightarrow S_f$ $(\mu_{0i} \cdot \mu_{ij} \cdot \mu_{jf})$, (II) $S_0 \rightarrow S_f \rightarrow S_0 \rightarrow S_f$ $(\mu_{0f} \cdot \mu_{0f} \cdot \mu_{0f})$, (III) $S_0 \rightarrow S_i \rightarrow S_i \rightarrow S_f$ $(\mu_{0i} \cdot \Delta\mu_{00}^{ij} \cdot \mu_{jf})$, (IV) $S_0 \rightarrow S_i \rightarrow S_f \rightarrow S_f$ $(\mu_{0i} \cdot \mu_{jf} \cdot \Delta\mu_{00}^{ff})$, (V) $S_0 \rightarrow S_f \rightarrow S_f \rightarrow S_f$ $(\mu_{0f} \cdot \Delta\mu_{00}^{ff} \cdot \Delta\mu_{00}^{ff})$. The transition dipole moments, μ, and dipole moment difference between excited and ground state, $\Delta\mu$, involved in the transition paths are given in the parenthesis. Among them, path (II) is present in both symmetrical and asymmetrical systems, and for symmetrical molecules, the last three channels, (III)–(V), should vanish [14]. For the conjugated charge-transfer molecules studied here, one can easily see that path (II) is an important contributor, which is proportional to the third power of the transition moment between ground and final states. In other words, a strong one-photon absorption (OPA) state can be a strong 3PA state as well. In addition, from another point of view, there is only one transition ($S_0 \rightarrow S_1$) corresponding to the three-photon transition (28,195 cm^{-1}) of 1064 nm. Although such semi-empirical calculations are not very definitive, we regard the results as strong evidence that the first excited state, S_1, proved to be the strongest 3PA state as well as the strongest OPA state.

The only distinguish in molecular structure between BASF and BMOSF is that they have different donor groups (D). According to Hammett equation [22–24], the substituent constant (σ) can be used to determine donor strength. The σ value for p-substituted-amino group (–NH_2) is −0.66, and the corresponding value for p-substituted-methoxyl group (–OCH_3) is −0.268 [25–27]. So the electron-donating strength should be in the order: amino group > methoxyl group. Correlating the strength of donor with 3PA cross-sections, however, we have found that the 3PA cross-sections are not in proportion to the donor strength. For example, BMOSF exhibits larger σ_3' value although methoxyl group possesses weak electron-donating ability. The charge density distributions of BASF and BMOSF in both ground- and excited-state were calculated by using PM3 semi-empirical method. Take BASF for example, the result was shown in Fig. 3, which indicates clearly that the substantial symmetric charge redistribution occurs upon excitation. The variation of charge density

Table 1
Electronic transition data obtained by the ZINDO/S semiempirical method for BASF at the PM3 optimized geometry

Electronic transitions	Transition energy (cm^{-1})	f	MO/character	Transition dipole moment (a.u.[b])		
				X[a]	Y	Z
$S_0 \rightarrow S_1$	27826.5	2.4267	HOMO → LUMO (92%)	5.349	−0.298	0.072
$S_0 \rightarrow S_2$	32665.9	0.0346	HOMO → LUMO + 5 (61%) HOMO − 3 → LUMO (46%)	−0.017	0.589	−0.036
$S_0 \rightarrow S_3$	32831.0	0.0656	HOMO → LUMO + 1 (66%) HOMO − 1 → LUMO (58%)	−0.165	−0.793	0.047
$S_0 \rightarrow S_4$	33471.7	0.0461	HOMO − 4 → LUMO (45%)	0.628	−0.242	0.021
$S_0 \rightarrow S_5$	34061.1	0.0373	HOMO − 1 → LUMO + 3 (46%) HOMO → LUMO + 4 (39%)	0.176	−0.572	0.039
$S_0 \rightarrow S_6$	34075.0	0.0029	HOMO − 1 → LUMO + 4 (46%)	−0.130	−0.107	0.005
$S_0 \rightarrow S_7$	38420.2	0.2269	HOMO − 1 → LUMO + 1 (57%) HOMO → LUMO + 2 (54%)	−1.381	0.190	−0.032
$S_0 \rightarrow S_8$	38974.2	0.0001	HOMO − 1 → LUMO (70%) HOMO → LUMO + 1 (56%)	0.027	−0.013	0.001
$S_0 \rightarrow S_9$	42045.1	0.0132	HOMO − 2 → LUMO (66%) HOMO → LUMO + 2 (62%)	−0.317	−0.047	−0.016
$S_0 \rightarrow S_{10}$	42517.0	0.0011	HOMO − 1 → LUMO + 2 (52%)	0.015	0.090	−0.001

[a] X is the long molecular axis.
[b] a.u. is atomic units [15].

Table 2
Electronic transition data obtained by the ZINDO/S semiempirical method for BMOSF at the PM3 optimized geometry

Electronic transitions	Transition energy (cm^{-1})	f	MO/character	Transition dipole moment (a.u.[b])		
				X[a]	Y	Z
$S_0 \rightarrow S_1$	27841.2	2.4197	HOMO → LUMO (92%)	5.347	−0.155	0.0003
$S_0 \rightarrow S_2$	32482.3	0.0093	HOMO → LUMO + 5 (69%) HOMO − 3 → LUMO (53%)	−0.049	0.304	0.0000
$S_0 \rightarrow S_3$	32854.7	0.0883	HOMO → LUMO + 1 (75%) HOMO − 1 → LUMO (61%)	−0.206	−0.918	−0.0003
$S_0 \rightarrow S_4$	33275.7	0.0528	HOMO − 4 → LUMO (43%)	0.647	−0.322	−0.0002
$S_0 \rightarrow S_5$	33969.7	0.0390	HOMO − 1 → LUMO + 3 (56%) HOMO → LUMO + 4 (51%)	0.107	−0.606	−0.0001
$S_0 \rightarrow S_6$	33999.7	0.0049	HOMO − 1 → LUMO + 4 (54%) HOMO → LUMO + 3 (52%)	−0.120	−0.181	0.0003
$S_0 \rightarrow S_7$	38589.2	0.2463	HOMO − 1 → LUMO + 1 (57%) HOMO → LUMO + 2 (57%)	−1.425	0.268	0.0007
$S_0 \rightarrow S_8$	38786.8	0.0003	HOMO − 1 → LUMO (70%) HOMO → LUMO + 1 (54%)	0.048	−0.024	0.0001
$S_0 \rightarrow S_9$	41863.8	0.0320	HOMO − 2 → LUMO (68%) HOMO → LUMO + 2 (58%)	−0.501	−0.028	0.0001
$S_0 \rightarrow S_{10}$	42780.7	0.0005	HOMO − 1 → LUMO + 2 (50%)	−0.042	0.044	−0.0003

[a] X is the long molecular axis.
[b] a.u. is atomic units [15].

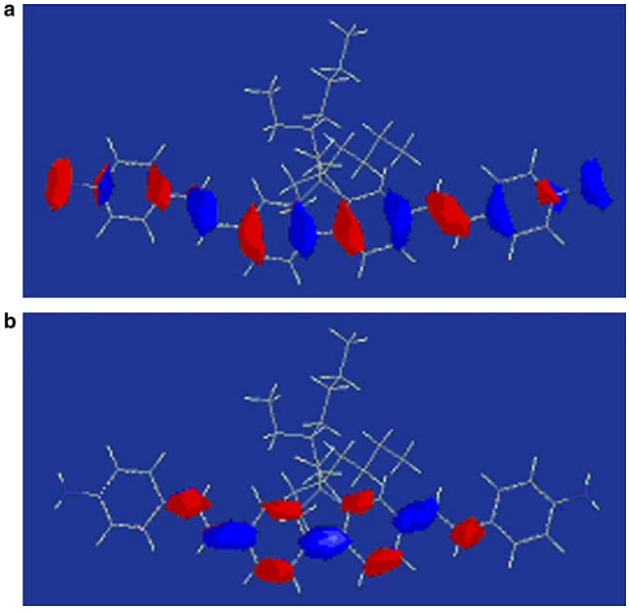

Fig. 3. Charge density distributions of BASF in (a) HOMO and (b) LUMO.

distribution reflects the extent of intramolecular charge transfer. The structure of the skeleton can be divided into three parts: ρ_1, ρ_1', and ρ_2 (see Fig. 4). Here, ρ_1

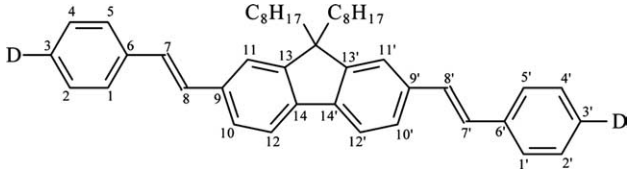

Fig. 4. Atom labeling scheme for molecules studied in this Letter.

and ρ_1' describe the average charge densities on atoms C1–C5 and C1′–C5′, respectively, while ρ_2 describes the corresponding average value for atoms on the conjugating bridge (C6–C6′). The charge density difference between the first excited state (S_1) and ground state (S_0), $\Delta\rho_1/\Delta\rho_2/\Delta\rho_1'$, is thus an intramolecular charge transfer character. The unit of charge on every atom is e. The related data are presented in Table 3. Obviously, there is no obvious distinction for the ground-state charge densities ρ_2, and they are all closed to $-2.24e$. While, the charge densities ρ_1 and ρ_1' exhibit different values due to the different donor strength. The ρ_1 or ρ_1' of BASF are closed to $-0.84e$, yet the corresponding values of BMOSF are $-0.69e$. But once in the excited states, charge redistributions distinctively occur. The charge density difference $(\Delta\rho_1/\Delta\rho_2/\Delta\rho_1')$ for BMOSF is $+0.3218e/+1.0138e/+0.3237e$, clearly larger than

Table 3
Three-photon absorption cross-sections (σ_3') and the charge density distributions of ground- and excited-state ($\rho_1/\rho_2/\rho_1'$)

Molecules	3PA cross-sections σ_3' ($\times 10^{-78}$ cm^6 s^2)	$\rho_1/\rho_2/\rho_1'(e)$	$\Delta\rho_1/\Delta\rho_2/\Delta\rho_1'(e)$
BASF	84	−0.8410/−2.2393/−0.8412 (S_0) −0.6016/−1.8322/−0.6024 (S_1)	+0.2394/+0.4071/+0.2388
BMOSF	114	−0.6905/−2.2422/−0.6907 (S_0) −0.3687/−1.2284/−0.3670 (S_1)	+0.3218/+1.0138/+0.3237

that for BASF, $\Delta\rho_1/\Delta\rho_2/\Delta\rho_1' = +0.2394e/+0.4071e/+0.2388e$, as indicated that the extent of symmetric intramolecular charge transfer occurred in BMOSF is larger than BASF, so the value of σ_3' for BMOSF is relatively larger. Evidently, substantial charge redistribution occurs upon excitation, and intramolecular charge transfer has great effects on 3PA cross-sections.

4. Conclusions

In summary, 3PA of two novel symmetrical charge transfer fluorene-based molecules, BASF and BMOSF, was demonstrated at 1064 nm. The measured 3PA cross-sections are 84×10^{-78} and 114×10^{-78} $cm^6\ s^2$ for BASF and BMOSF, respectively. We did not find that the 3PA cross-sections are in proportion to the donor strength in the experiment. Electronic transitions and charge density distribution of two molecules were calculated by the ZINDO/S and PM3 semi-empirical method, respectively. The experimental and theoretical results demonstrated that the first excited state, S_1, is the strongest 3PA state for both two molecules, and the extent of symmetric intramolecular charge transfer ($\Delta\rho_1/\Delta\rho_2/\Delta\rho_1'$) has a significant effect on the 3PA cross-section, which increases with an increase in the $\Delta\rho_1/\Delta\rho_2/\Delta\rho_1'$ value.

Acknowledgements

This work is supported by the National Science Foundation of China (No. 60207005) and The Shanghai Science & Technology Development Foundation (No. 012261068).

References

[1] M. Göppert-Mayer, Ann. Phys. 9 (1931) 373.
[2] M. Albota, D. Beljonne, J.-L. Bré zdas, J.E. Ehrlich, J. Fu, A.A. Heikal, S.E. Hess, T. Kogej, M.D. Levin, S.R. Marder, D. McCord-Maughon, J.W. Perry, H. Rockel, M. Rumi, G. Subramaniam, W.W. Webb, X. Wu, C. Xu, Science 281 (1998) 1635.
[3] B.H. Cumpston, S.P. Ananthavel, S. Barlow, D.L. Daniel, J.E. Ehrlich, L.L. Erskine, A.A. Heikal, S.M. Kuebler, I.-Y.S. Lee, D. McCord-Maughon, J. Qin, H. Röckel, M. Rumi, X.L. Wu, S.R. Mader, J.W. Perry, Nature 398 (1999) 51.
[4] W. Zhou, S.M. Kuebler, K.L. Braun, T. Yu, J.K. Cammack, C.K. Ober, J.W. Perry, S.R. Mader, Science 296 (2002) 1106.
[5] M. Gu, Opt. Lett. 21 (1996) 988.
[6] S. Maiti, J.B. Shear, R.M. Williams, W.R. Zipfel, W.W. Webb, Science 275 (1997) 530.
[7] R. Naskrecki, M. Menard, P. VanderMeulen, G. Vigneron, S. Pommeret, Opt. Commun. 153 (1998) 32.
[8] G.S. He, P.P. Markowicz, T.-C. Lin, P.N. Prasad, Nature 415 (2002) 767.
[9] G.S. He, J.D. Bhawalkar, P.N. Prasad, Opt. Lett. 20 (1995) 1524.
[10] C. Zhan, D. Li, D. Zhan, Y. Li, D. Wang, T.X. Wang, Z.Z. Lu, L.Z. Zhao, Y.X. Nie, D.B. Zhu, Chem. Phys. Lett. 353 (2002) 138.
[11] D. Wang, C. Zhan, Y. Chen, Y.J. Li, Z.Z. Lu, Y.X. Nie, Chem. Phys. Lett. 369 (2003) 621.
[12] P.N. Prasad, Mol. Cryst. Liquid Cryst. 415 (2004) 1.
[13] F.E. Hernández, K.D. Belfield, I. Cohanoschi, Chem. Phys. Lett. 391 (2004) 22.
[14] P. Cronstrand, Y. Luo, P. Norman, Hans. Ågren, Chem. Phys. Lett. 375 (2003) 233.
[15] W. Ma, Y. Wu, J. Han, D. Gu, F. Gan, Chem. Phys. Lett. 403 (2005) 405.
[16] K.D. Belfield, D.J. Hagan, E.W.V. Stryland, K.J. Schafer, R.A. Negres, Org. Lett. 1 (1999) 1575.
[17] J.J.P. Srewar, J. Comput. Chem. 209 (1989) 221.
[18] J. Ridley, M.C. Zerner, Theor. Chim. Acta 32 (1973) 111.
[19] C. Forber, M.C. Zerner, J. Am. Chem. Soc. 107 (1985) 5884.
[20] K.D. Belfield, M.V. Bondar, O.V. Przhonska, K.J. Schafer, W. Mourad, J. Fluoresc. 97 (2002) 141.
[21] G.A. Reynolds, K.H. Drexhage, Opt. Commun. 13 (1975) 222.
[22] L.P. Hammett, J. Am. Chem. Soc. 59 (1937) 96.
[23] L.P. Hammett, Chem. Rev. 17 (1935) 125.
[24] L.P. Hammett, J. Chem. Educ. 43 (1966) 464.
[25] C.G. Swain, E.C. Lupton, J. Am. Chem. Soc. 90 (1968) 4328.
[26] P.R. Wells, Linear Free Energy Relationships, Academic Press, New York, 1968.
[27] J.E. Leffler, E. Grunwald, Rates and Equilibria of Organic Reactions, Wiley, New York, 1963.